Observation of the Fano-Kondo Anti-Resonance in a Quantum Wire with a Side-Coupled Quantum Dot

Masahiro Sato, Hisashi Aikawa, Kensuke Kobayashi, Shingo Katsumoto, and Yasuhiro Iye
Institute for Solid State Physics, University of Tokyo, 5-1-5 Kashiwanoha, Chiba 277-8581, Japan
(Dated: October 4, 2004)

We have observed the Fano-Kondo anti-resonance in a quantum wire with a side-coupled quantum dot. In a weak coupling regime, dips due to the Fano effect appeared. As the coupling strentgh increased, conductance in the regions between the dips decreased alternately, showing the growth of the Kondo state. From the temperature dependence and the response to the magnetic field, we conclude that the conductance reduction is due to the Fano-Kondo anti-resonance. At a Kondo valley with the Fano parameter $q \approx 0$, the phase shift at a quantum dot stays constant over the range of gate voltage where the system is close to the unitarity limit.

PACS numbers: 72.15.Qm, 73.21.La, 73.23.Hk

The experimental realization of the Kondo effect [1] in a semiconductor quantum dot has opened up a new human-made stage to investigate many body effects [2]. In a previous paper, we have shown that spin-scattering at a quantum dot leads to quantum decoherence [3]. This means that the creation of a spin-entangled state between a localized spin and a conduction electron causes quantum decoherence [4]. At the same time, however, such an entangled state is a starting point to build an expression of the Kondo singlet [5], which is obtained by replacing the wave functions of single-particles with those of quasi-particles. In the Kondo singlet states, the coherence of electrons is recovered. Such recovery of quantum coherence comes from the asymptotic strong-coupling in the Kondo effect.

The direct evidence for the coherence of the Kondo state is the interference effect through a quantum dot in the Kondo state. Ji *et al.* measured the phase shift of electrons through a dot in the Kondo state in an Aharonov-Bohm (AB) ring which is a representative interferometer in electronic transport [6]. They found that the phase shift significantly varies even on the Kondo plateau of conductance, which may suggest the breakdown of the Anderson model approximation of a quantum dot. However, the difficulty in measuring the phase shift in AB geometry is pointed out [7], and experiments in simpler structures such as a stub-resonator (a schematic diagram is shown in Fig. 1(a)) [8, 9] are desired. An experiment in such geometry is also important to investigate the Kondo interpretation of the 0.7 anomaly in quantum point contacts [10].

Some of the present authors have reported the observation of the Fano anti-resonance in a quantum wire with a side-coupled quantum dot [11], which is a kind of a stub-resonator. The Fano effect [12] is a consequence of interference between a localized state and a continuum, which correspond to a state in the side-coupled dot and that in the wire, respectively. The Fano effect appears as a characteristic line shape of transition probability, which is proportional to the conductance G of the system. The line shape is expressed as

$$G(\epsilon) \propto \frac{(\epsilon + q)^2}{\epsilon^2 + 1}, \tag{1}$$

where ϵ is the energy difference from the resonance position normalized with the width of the resonance, and q is Fano's asymmetric parameter [13]. The Fano parameter represents the degree of distortion and $q = 0$ corresponds to an anti-resonance dip. The Fano-Kondo effect – the Fano effect which appears in the Kondo cloud – is hence sensitive to coherence and phase shifts [14]. In this Letter, we report the observation of the Fano-Kondo anti-resonance in a quantum wire with a side-coupled quantum dot. Phase shift locking to $\pi/2$ is deduced from the analysis of the line shape of the anti-resonance.

Our device consists of a quantum dot and a quantum wire difined in a two-dimensional electron gas (2DEG, sheet carrier density 3.8×10^{15} m^{-2}, mobility 80 m^2/Vs) formed at a GaAs/AlGaAs hetero-structure. Au/Ti metallic gates were deposited as shown in Fig. 1(b). A quantum dot is defined by the upper three gates and the two gates marked as "M" (M-gates). The lower three gates adjust the conductance of the wire. The middle of the upper gate is used to control the potential of the dot (gate voltage $V_{\rm g}$) and M-gates tune the coupling between the dot and the wire (gate voltage $V_{\rm m}$). Tuning the coupling strength by M-gates inevitably induces the electrostatic potential shift of the dot, whereas the potential shift by $V_{\rm g}$ causes little change in the coupling strength. Accordingly, the potential shift by $V_{\rm m}$ can be compensated by $V_{\rm g}$ (approximately $\Delta V_{\rm g} = -4.5\Delta V_{\rm m}$ in the present sample). For the sake of a simpler description, we henceforth redefine $V_{\rm g} \equiv V_{\rm g}({\rm raw}) - (V_{\rm m} - 0.846)$, *i.e.*, the value of $V_{\rm g}$ renormalized to the value at $V_{\rm m} = -0.846$ V. In order to attain a large value of Kondo temperature $T_{\rm K}$, the device was designed to make the dot size smaller than that used in Ref. [11]. The dot is placed close to the wire to avoid temperature dependence associated with a change of the coherence length, which is unfavorable for the present study. Although the proximity of the dot to

the wire would cause a Fano-charging mixing effect [15], it is less severe in a comparatively strong coupling regime explored here. The sample was cooled in a dilution refrigerator down to 30 mK and was measured by standard lock-in techniques in a two-terminal setup.

In order to obtain the relevant parameters of the dot, we first measured the direct charge transport through the dot. We slightly opened the left one of the side gates of the dot and pinched off the left one of the lower three gates. We measured the current from the upper left lead through the quantum dot to the lower right lead. The average level spacing Δ obtained from excitation spectroscopy is about 0.3 meV, which gives the dot diameter as about 170 nm and the total number of electrons as about 90. The electron temperature estimated from the widths of resonance peaks followed the fridge temperature down to 100 mK and severe saturation occurred below that. We expect that the parameters of the side-coupled dot are nearly the same as the parameters described above, though some amount of difference is inevitable. Then the direct connection was pinched off by the side gate and the wire was formed by the lower three gates. The wire conductance far from resonances was adjusted to be around $G_q \equiv 2e^2/h$, *i.e.*, at the first step of the conductance staircase.

Figure 1(c) shows the wire conductance against $V_{\rm g}$ at various coupling strength adjusted by $V_{\rm m}$. In a weak coupling regime (at the top of Fig. 1(c)), Coulomb "dips" appear, reproducing the previous result [11]. This is due to the destructive interference, *i.e.*, the Fano anti-resonance. As the coupling strength increases, conductance in the regions between the dips (Coulomb valleys) decreases alternately. These reductions of the conductance connect two neighboring dips into one (in regions A and B). We have observed four such valleys (as will be shown in Fig. 2) where the conductance decreases as the coupling strength increases. In the following, we first confirm that these reductions are due to the Fano-Kondo anti-resonance, then discuss the information obtained from the experiments.

The upper panel of Fig. 2 shows the zero-bias wire conductance as a function of $V_{\rm g}$ at three different temperatures for a medium coupling strength ($V_{\rm m} = -0.846$ V). The closed bars indicate the positions of the Coulomb dips. For valley B, the positions cannot be resolved directly and are extrapolated from the positions at $V_{\rm m} = -0.886$ V. In the four regions ("Kondo valleys") indicated by A-D, conductance decreases with decreasing temperature. The Kondo effect emerges for a quantum dot with odd number of electrons with a few exceptions [16]. Hence it usually appears alternately at Coulomb valleys as we observed at Kondo valleys A-D.

The distances between the Coulomb dips are shorter at the Kondo valleys than those at the neighboring valleys. The level spacing Δ obtained from this difference of the distances is in good agreement with Δ obtained from excitation spectroscopy. This means the simple "spin-pair" picture holds for these valleys and the conditions for the Kondo effect are fulfilled at valleys A-D.

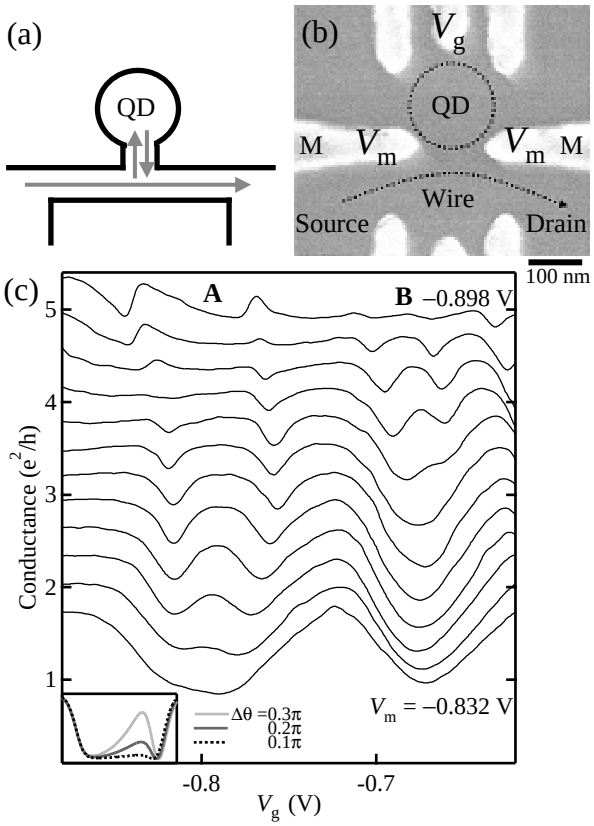

FIG. 1: (a) Schematic diagram of a stub-resonator. (b) Scanning electron micrograph of the device. The white areas are metallic gates made of Au/Ti. The dot and the wire are indicated by dotted lines. (c) Conductance of the wire measured at several coupling strength tuned by $V_{\rm m}$. The step in $V_{\rm m}$ is 6 mV and the data are offset by $0.3e^2/h$ for clarity. Inset: Calculated conductance shapes. The phase shift are assumed to vary at the Kondo valley. The phase shift variations $\Delta\theta$ were set to be 0.1π, 0.2π, 0.3π. The scales are adjusted to compare with Kondo valley A.

The lower panel of Fig. 2 is a color scale plot of the conductance on the plane of $V_{\rm g}$ and the source-drain bias voltage $V_{\rm sd}$. The conductance drops around $V_{\rm sd} = 0$ mV at the Kondo valleys. We should be careful that the dot is "side-coupled" and $V_{\rm sd}$ is not directly applied to the dot but to the wire. The wire by itself can show nonlinear conductance [17]. In this experiment, however, the non-linearity of the wire is small, because the wire is under the plateau condition and the scale of $V_{\rm sd}$ in the lower panel of Fig. 2 is magnitute smaller than $V_{\rm sd}$ in the previous reports [10, 17]. Furthermore, the response to $V_{\rm g}$ and the reversed Coulomb diamond like structure (not well resolved in Fig. 2) indicate that the zero-bias 'dips" originate from the Kondo effect of the dot. The charging energy U estimated from the reversed Coulomb diamond ranges from 0.3 to 0.5 meV.

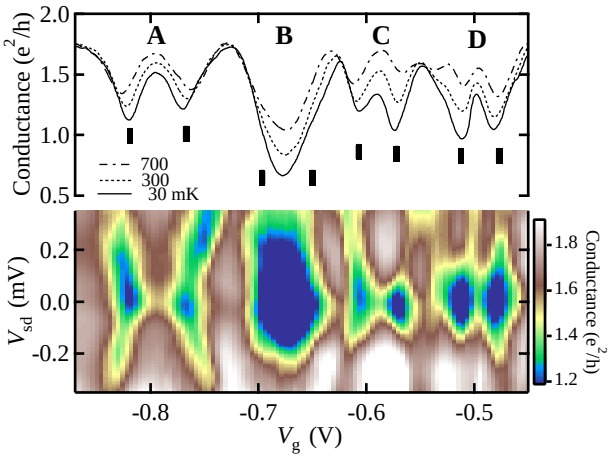

FIG. 2: Upper: Zero-bias conductance of the quantum wire at three different temperatures as a function of the gate voltage V_g at $V_m = -0.846$ V. The bars indicate the positions of Coulomb "dips" and A-D indicate the Coulomb valleys where the Kondo effect emerges. Lower: Color scale plot of the conductance on the V_g-V_{sd} plane. Both the upper and the lower panels use the same V_g axis.

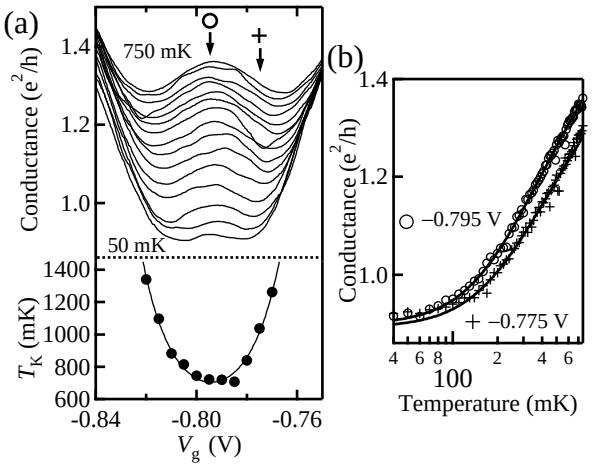

FIG. 3: (a) Upper: Conductance as a function of gate voltage at temperatures from 750 mK to 50 mK with the temperature step of 50 mK. Lower: Kondo temperatures T_K obtained from the temperature dependence. (b) Examples of the fitting to obtain T_K. The gate voltages adopted here are indicated by arrows in (a).

The upper panel of Fig. 3(a) shows detailed temperature dependence of $G(V_g)$ at Kondo valley A. We obtained the Kondo temperature T_K by fitting an empirical function [18]:

$$G(T) = G_0 - G_1 \left(\frac{T_K'^2}{T^2 + T_K'^2} \right)^s, \qquad (2)$$

where G_1, $T_K' \equiv T_K/\sqrt{2^{1/s} - 1}$ and s are fitting parameters. G_0 was fixed to $1.8e^2/h$, which is the wire conductance far from the anti-resonance. Examples of the fitting are shown in Fig. 3(b). Note that we do not take the data below 120 mK into the fitting considering the saturation of electron temperature. From the fitting, $s = 0.25 \pm 0.04$ was obtained, which is in accordance with the prediction for spin 1/2 impurities. The obtained T_K are plotted against V_g in the lower panel of Fig. 3(a). T_K depends parabolically on V_g with the bottom around the mid-point of the Kondo valley just like the previous reports [19]. This dependence agrees well with the first order expansion of the Kondo temperature, $T_K = \sqrt{\Gamma U}\exp(\pi\epsilon(\epsilon + U)/\Gamma U)/2$, where Γ is the dot-wire coupling and ϵ is the single electron level measured from the Fermi level. We obtained $U = 0.36 \pm 0.03$ meV and $\Gamma = 0.32 \pm 0.02$ meV by fitting the above parabolic function to T_K. The obtained U corresponds with the value estimated from the reversed Coulomb diamond ($U = 0.33$ meV at this valley).

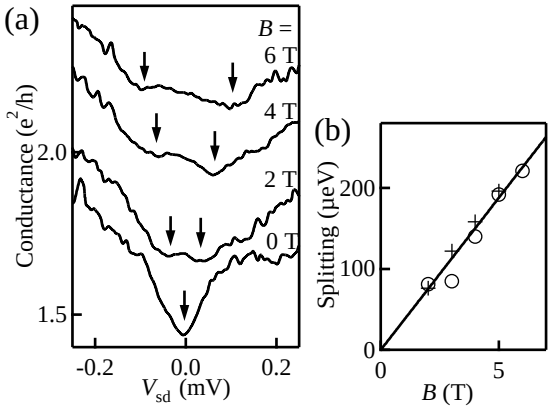

FIG. 4: (a) Conductance versus V_{sd} at Kondo valley A under various magnetic fields up to 6 T. The arrows indicate the positions of the conductance dips. (b) Distance between two dip positions versus the magnetic field. The data were taken at Kondo valleys A (open circles) and C (crosses) in Fig. 2. The line corresponds to $|g| = 0.33$.

Figure 4(a) shows the splitting of the zero-bias conductance dip under the external magnetic field parallel to the 2DEG plane. The splitting is simply proportional to the field as shown in Fig. 4(b). This can be attributed to the Zeeman splitting of the Kondo anomaly. From the slope of the fitted line, we obtain the g-factor of electrons as $|g| = 0.33$, which is close to that reported for GaAs/AlGaAs 2DEG [20].

So far we have confirmed that the conductance reduction in regions A-D in Fig. 2 is due to the Fano-Kondo anti-resonance. Because the side gates of the dot is completely pinched off, only destructive interference can cause the conductance reduction. The observation of the Kondo effect through the pure interference effect manifests that electron transport through the Kondo cloud is coherent as predicted [8].

In Fig. 1(c), two dips merges into one in regions A and B. This means the system almost reaches the unitarity limit [19]. This is consistent with the obtained $T_{\rm K}$ shown in the lower panel of Fig. 3. The residual conductance at the "unitarity limit" Kondo valleys (*e.g.*, $0.7e^2/h$ at valley B in Fig. 2 and $0.9e^2/h$ at valley A in Fig. 3) is probably due to the finite area between the wire and the dot. This area itself works as a resonator and spoils the perfect reflection [9], while the phase shift is unchanged because $q \approx 0$ in the present case.

When the coupling is weak (at the top of Fig. 1(c)), the two dips at both sides of valley A have asymmetric Fano line shapes ($q \neq 0$). It has been anticipated that symmetry of transport through a quantum dot is dominated by a few states with an anomalously strong coupling to an electrode (strong coupling states, SCSs) [21], and we experimentally demonstrated the prediction [22]. In a weak coupling regime, the q's of the two dips at both sides of valley A are determined by an SCS. As the coupling strength increases, however, the values of q approach to zero. This indicates that the coupling strength is renormalized by the Kondo many-body effect, and the Kondo state takes over the SCS in the weak coupling regime.

In a strong coupling regime (at $V_{\rm m} = -0.832$ V in Fig. 1(c)), q is nearly zero and the Kondo valleys are almost in the unitarity limit. Kondo valley A has a line shape similar to that observed in the unitarity limit of the direct transport [19]. If the phase shift varies at the Kondo valley, a line shape of a valley should be distorted. We compared the observed line shape with the calculated line shapes. We used a simple S-matrix model presented in Ref. [11]. An artificial phase shifter which causes phase locking and a phase shift variation was incorporated in the model. Some calculated line shapes are shown in the inset of Fig. 1(c). From the comparison, the variation in the phase shift is estimated to be less than 0.15π. This is in accordance with the existing theories which predict the locking of the phase shift in the unitarity limit. At Kondo valley A with $q \approx 0$, the phase shift locking occurs around the minima of the conductance. This means the locked value is around $\pi/2$. Our result is in contrast to the previous result [6]. The discrepancy may come from the difference in the setup of interferometers, though we have no convincing explanation at present.

The zero-bias anomaly appeared as shown in Fig. 2, despite that no voltage was directly applied to the dot in the present configuration. The Kondo cloud is affected by $V_{\rm sd}$ applied to the wire, probably because the Kondo cloud spreads into the wire. This is reasonable considering the size of the Kondo cloud $\hbar v_{\rm F}/k_{\rm B}T_{\rm K}$ ($v_{\rm F}$: Fermi velocity), which exceeds 2 μm for $T_{\rm K}$ less than 1 K [23]. The present structure provides means to investigate the size of the Kondo cloud.

In summary, we have observed the Fano-Kondo anti-resonance in a quantum wire with a side-coupled dot. Phase shift locking to $\pi/2$ is deduced from the line shape of the anti-resonance.

This work is supported by a Grant-in-Aid for Scientific Research and by a Grant-in-Aid for COE Research from the Ministry of Education, Culture, Sports, Science, and Technology of Japan.

[1] J. Kondo, in *Solid State Physics* Vol. 23, p. 13, eds. H. Ehrenreicht, F. Seitz, and D. Turnbull (Academic Press, New York, 1969).
[2] D. Goldhaber-Gordon *et al.*, Nature **391**, 156 (1998); S. M. Cronenwett *et al.*, Science **281**, 540 (1998); J. Schmid *et al.*, Physica (Amsterdam) **256B-258B**, 182 (1998).
[3] H. Aikawa *et al.*, Phys. Rev. Lett. **92**, 176802 (2004).
[4] J. König and Y. Gefen, Phys. Rev. Lett. **86**, 3855 (2001); Phys. Rev. B **65**, 045316 (2002).
[5] K. Yosida and A. Yoshimori, *Magnetism V*, edited by H. Suhl (Academic Press, 1973).
[6] Y. Ji *et al.*, Science **290**, 779 (2000); Y. Ji, M. Heiblum, and H. Shtrikman, Phys. Rev. Lett. **88**, 076601 (2002).
[7] A. Aharony *et al.*, Phys. Rev. B **66**, 115311 (2002).
[8] K. Kang *et al.*, Phys. Rev. B **63**, 113304 (2001); A. A. Aligia and C. R. Proetto, Phys. Rev. B **65**, 165305 (2002); M. E. Torio, *et al.*, Phys. Rev. B **65**, 085302 (2002).
[9] W. B. Thimm, J. Kroha, and J. von Delft, Phys. Rev. Lett. **82**, 2143 (1999).
[10] Y. Meir, K. Hirose, and N. S. Wingreen, Phys. Rev. Lett. **89**, 196802 (2002); S. M. Cronenwett *et al.*, Phys. Rev. Lett. **88**, 226805 (2002).
[11] K. Kobayashi *et al.*, Phys. Rev. B **70**, 035319 (2004).
[12] U. Fano, Phys. Rev. **124**, 1866 (1961).
[13] K. Kobayashi *et al.*, Phys. Rev. Lett. **88**, 256806 (2002); Phys. Rev. B **68**, 235304 (2003).
[14] W. Hofstetter, J. König, and H. Schöller, Phys. Rev. Lett. **87**, 156803 (2001).
[15] A. C. Johnson *et al.*, Phys. Rev. Lett. **93**, 106803 (2004).
[16] J. Schmid *et al.*, Phys. Rev. Lett. **84**, 5824 (2000); S. Sasaki *et al.*, Nature **405**, 764 (2000).
[17] A. Kristensen *et al.*, Phys. Rev. B **62**, 10950 (2000).
[18] T. A. Costi, A. C. Hewson, and V. Zlatic, J. Phys. Condens. Matter **6**, 2519 (1994); D. Goldhaber-Gordon *et al.*, Phys. Rev. Lett. **81**, 5225 (1998).
[19] W. G. van der Wiel *et al.*, Science **289**, 2105 (2000).
[20] H. W. Jiang and E. Yablonovitch, Phys. Rev. B **64**, 041307 (2001).
[21] P. G. Silvestrov and Y. Imry, Phys. Rev. Lett. **85**, 2565 (2000); A. L. Yeyati and M. Büttiker, Phys. Rev. B **62**, 7307 (2000); T. Nakanishi, K. Terakura, and T. Ando, Phys. Rev. B **69**, 115307 (2004).
[22] H. Aikawa *et al.*, cond-mat/0312431.
[23] P. Simon and I. Affleck, Phys. Rev. B **68**, 115304 (2003).